DIVISION S-5—PEDOLOGY

Modeling Soil–Landscape and Ecosystem Properties Using Terrain Attributes

P. E. Gessler,* O. A. Chadwick, F. Chamran, L. Althouse, and K. Holmes

ABSTRACT

Soil–landscape patterns result from the integration of short- and long-term pedogeomorphic processes. A 2-ha hillslope catena in California shows short-distance variation in A horizon depth from 8 to 80 cm and in soil depth from 8 to >450 cm in convex to concave positions. Similar variations in net primary productivity (NPP) and soil C represent significant information often not captured by soil survey maps. Strong correlations between these measured soil–landscape variables and explanatory digital terrain attributes are used to develop quantitative soil–landscape models. We were able to account for between 52 and 88% of soil property variance using easily computed terrain variables such as slope and flow accumulation. Spatial implementation of the models suggest lateral redistribution processes resulting in differential accumulation of C and soil mass in convergent and divergent landscape positions. The models are explicit and quantitative, which enables their use for testing hypotheses about the spatial distribution of fine-scale landscape and ecosystem processes and for parameterizing spatially distributed hydrological and ecosystem simulation models.

THE UNDERSTANDING that topography modifies water flow and material redistribution processes and resulting ecosystem and soil patterns in landscapes lies at the heart of the catena concept (Milne, 1935, 1936). It has been reformulated and modified by numerous studies (Conacher and Dalyrymple, 1977; Hole and Campbell, 1985; Dikau, 1989; Moore et al., 1993; Gessler et al., 1995; Sommer and Schlichting, 1997) often with the aim of refining a conceptual framework for soil mapping or landscape process monitoring and interpretation (Simonson, 1959; Smeck et al., 1983).

The advent of geographic information system (GIS)-based digital elevation modeling has facilitated quantitative modeling of catenas at local hillslope scales (McSweeney et al., 1994). Moore et al. (1993), building on the work of Speight (1968) and others, developed quantitative soil–landscape models using an integration of digital terrain analysis and statistical modeling methods to map predicted soil properties for a small hillslope in Colorado. In Australia, this work was continued and expanded to a broader suite of parent materials and geomorphic settings to test an integration of tools for digital terrain analysis, field sampling, remote sensing, statistical modeling, and GIS (Gessler et al., 1995, 1996; Gessler, 1996; McKenzie et al., 2000). These workers demonstrated the successful implementation of quantitative soil–landscape modeling on a broad landscape scale useful for soil resource inventory and as a framework for understanding soil–landscape function. Moore et al. (1993) and Gessler et al. (1995) showed strong correlation and predictive utility between a digital terrain index, the compound topographic index (CTI), and several soil properties. The CTI, often referred to as the steady-state wetness index, is a quantification of catenary landscape position. It integrates both landform position and context through an index defined as

$$\mathrm{CTI} = \ln(A_s/\tan\beta) \qquad [1]$$

where A_s is the specific catchment area [area (m^2) per unit width orthogonal to the flow direction] and β is the slope angle. Small values of CTI generally depict upper catenary positions and large values lower catenary positions with an overall range typically from 2 to 12 for zero-order upland areas.

The purpose here was to continue development of the quantitative catena concept at the hillslope scale for a detailed study site in southern California. Whereas the earlier catena study by Moore et al. (1993) focused entirely on patterns of surficial soil properties (in the top 15 cm), we began the process of integrating catena patterns with pedologic processes. Specifically, we combined developed methods of digital terrain analysis, soil and ecosystem field sampling, statistical modeling, and pedological and geomorphological process interpretation.

Detailed hillslope characterization and modeling of digital terrain and soil property relationships is key to understanding the biogeochemical cycling of nutrient elements in terrestrial ecosystems because they often point to the spatial distribution of significant processes. Thus, one of our results is development of explicit soil–landscape models describing the distribution of ecosystem net primary production of C and soil C along the catena. The models provide preliminary context for developing hypotheses about soil–landscape function with respect to C cycling and water balance. We believe that understanding soil–landscape dynamics at the local hillslope catena level is key to understanding how to scale C dynamics to broader regional and global levels. In this paper, we provide a methodological blueprint for quantitative catena studies and results that have regional significance for soil survey and the biogeochemical interpretation of landscapes.

P.E. Gessler, Dep. of Forest Resources, Univ. of Idaho, Moscow, ID 83844-1133; O.A. Chadwick, F. Chamran, and K. Holmes, Dep. of Geography, Univ. of California, Santa Barbara, CA 93106; L. Althouse, Dep. of Ecology, Evolution & Marine Biology, Univ. of California, Santa Barbara, California, 93106. Received 28 Sept. 1999. *Corresponding author (paulg@uidaho.edu).

Published in Soil Sci. Soc. Am. J. 64:2046–2056 (2000).

Abbreviations: CEC, cation-exchange capacity; CTI, compound topographic index; C_{mass}, profile total C mass; DEM, digital elevation model; GIS, geographic information system; GPS, global positioning system; NPP, net primary productivity.

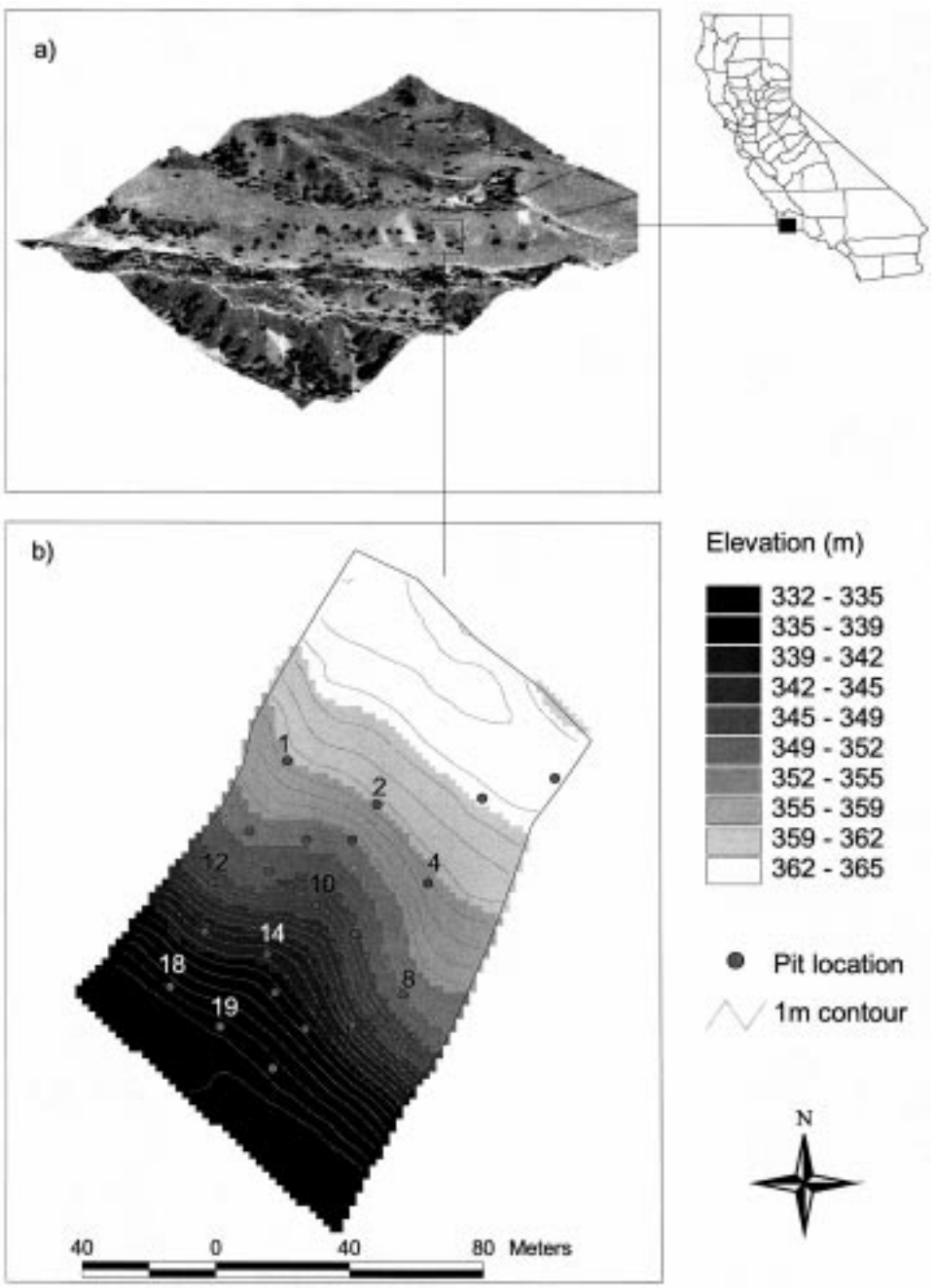

Fig. 1. Study site at the University of California Sedgwick Natural Reserve in Santa Barbara County, California. The study site is shown both (a) as a drape of a digital orthophoto over a 30-m digital elevation model and (b) with the individual soil pit locations displayed on a 1-m contour shade map of the hillslope.

MATERIAL AND METHODS

Study Site

The study area is located within the California Coast Range physiographic province in the Santa Ynez River Basin, Santa Barbara County, California (see Fig. 1). The University of California–Sedgwick Natural Reserve straddles the Santa Ynez Valley and San Rafael Mountains 45 km north of Santa Barbara. The Reserve is 2064 ha ranging in elevation from 320 to 732 m and has a Mediterranean climate with cool, wet winters and hot, dry summers. Average annual precipitation is 38 cm, but is highly variable. Summer temperatures often exceed 38°C and exhibit diurnal fluctuations up to 30°C (USDA-SCS, 1972). There is coastal fog intermittently throughout the year. The Reserve contains oak woodland, grassland, coastal sage scrub and riparian ecosystem assemblages. Common trees include valley oak (*Quercus lobata* Née) on the deep alluvial soils, with blue oak (*Quercus douglasii* Hook. & Arn.) and coast live oak (*Quercus agrifolia* Née) in canyons and hillslopes.

The catena study was established on a 2-ha zero-order watershed (i.e., ridges enclosing a hollow open at the lower end but having no incised channel) with the southwest aspect in an oak savanna. The watershed is cut into the side of a Quaternary terrace, and its upper reaches grade onto the planar terrace surface. The underlying geology is the Paso Robles formation, a weakly consolidated valley alluvium composed largely of

Monterey Shale deposited during the early Pleistocene by streams that drained the rising San Rafael Mountains. The soils are mapped as Chamise series (fine, mixed, active, thermic Typic, and Pachic Argixerolls; USDA-SCS, 1972). Hillslope elevations range from 332 to 365 m and slopes range from 0 to 66% and average 22%. The study area contains blue oak on steep terrain, and coast live oak in the colluvial hollow. The grassland vegetation is dominated by annual Mediterranean grasses such as ripgut brome (*Bromus diandrus* Roth), soft chess brome (*B. hordeaceus* L.), wild oat (*Avena barbata* Pott ex Link and *A. sativa* L.), and rat-tail fescue [*Vulpia myuros* (L.) C. Gmelin]. Herbaceous annuals are primarily exotic species that include filaree [*Erodium cicutarium* (L.) L'Hér.], black mustard [*Brassica nigra* (L.) Koch], tocolote (*Centaurea melitensis* L.), and a biennial mustard [*Hirschfeldia incana* (L.) Lagr.-Fossat]. Extremely well-drained xeric sites contain the native shrub saw-toothed goldenbush [*Hazardia squarrosa* (Hook. & Arn.) E. Greene]. Other native herbs include vinegar weed (*Trichostema lanceolatum* Benth.) and chia sage (*Salvia columbariae* Benth.).

Zero-Order Hillslope Geomorphometry and Sample Site Selection

The rectangular hillslope is ≈100 m wide by 200 m long encompassing both convex and concave landform components spanning from ridge top to valley bottom (Fig. 1). A Trimble GPS 4400 Total Station Survey system (Trimble, 1996) was used to collect an ≈5-m spacing regular grid of easting, northing, and elevation points by taking measurements along transects over the study site. The reported accuracy of the equipment and survey type is ±1 cm in the horizontal plane and ±2 cm vertically, relative to the accuracy of a local basestation. The basestation location was surveyed with three-dimensional accuracy of ≈2 cm (Holmes, 1999), indicating that the GPS points may have as much as ±5 cm of absolute error in three dimensions. Relative accuracies are better.

The point coordinates were processed using the ANUDEM interpolation software (Hutchinson, 1989, 1996) to develop five digital elevation models (DEMs) at grid point spacings of 2, 4, 6, 8, and 10 m. These were developed to compare the utility of digital terrain attributes for predicting soil patterns at different grid-point spacing resolutions. Primary and secondary terrain attributes (Moore et al., 1991) that quantify landform (e.g., slope gradient, profile and plan curvatures, flow direction, flow accumulation, CTI, and upslope mean statistics) were computed for each DEM using the TAPESG and UPSUMG software programs (Moore et al., 1993; Gessler et al., 1995; Gallant and Wilson, 1996). Terrain attributes provide a quantification of landform shape, connectivities and adjacencies that define external landscape geomorphometry and water flow patterns.

Histograms and summary statistics that characterize the distribution of the quantitative topographic attributes along with spatial displays were used to guide the distribution of 20 sample locations across the range of elevation, slope, and landform curvatures. These preliminary soil pits indicated that the surface soil patterns strongly reflected landform curvatures; therefore, a subset of nine sample locations (Fig. 1; Pits 1, 2, 4, 8, 10, 12, 14, 18, 19) encompassing this variation was chosen for soil pit excavation to bedrock or 3 m, whichever occurred first. An additional soil pit, located on the planar surface of the terrace at the top of the catena was not used in the hillslope modeling, but was used as an index of soil C content on relatively level ground. Depth to bedrock was determined directly in the backhoe and hand-dug pits. In concave positions where the soil material was >3 m in depth, estimations of soil depth were made using a truck-mounted Geoprobe that measures electrical resistivity of lithologic layers (Geoprobe Systems, 1995).

Soil Morphological Descriptions, Sampling, and Laboratory Analyses

Soil profiles were described using standard procedures (Soil Survey Staff, 1993) and horizons were channel sampled at several locations along pit faces for chemical and particle-size analyses. Intact clods (2–4 per horizon) were excavated from each horizon for bulk density measurement. Samples were oven-dried, crushed, sieved, and the >2-mm portion was weighed. Particle-size and chemical analyses were completed using the <2-mm fraction. Organic C and N were measured using a Fisons Instruments NA 1500 Series 2 CN analyzer (Fisons Scientific Equipment, Loughborough, UK) at the University of California–Santa Barbara. Bulk density was measured at University California–Santa Barbara by the saran coated clod method (Soil Survey Staff, 1996). Texture, pH, cation-exchange capacity (CEC) and base saturation analyses were completed by the University of Missouri Soil Analysis Lab. Particle size was measured by the pipette method (Soil Survey Staff, 1996). Soil pH was determined both by $CaCl_2$ and by water extract. Base concentrations and CEC were determined by the NH_4OAc method and CEC was also calculated as the sum of bases (Soil Survey Staff, 1996).

The mass of C in each horizon was calculated by multiplying the measured organic C percentage, corrected for gravel content, by the measured bulk density. Bulk density was determined as the mean of at least two clod samples per horizon. The mass of C was then multiplied by soil horizon thickness and added to provide an estimate of the mass of C stored (g cm^{-2}) in the entire soil profile. The profile C mass (C_{mass}) is a measure of the C stored in a 1-cm^2 area to the depth of the entire soil profile (A + B horizons).

Site Vegetation Sampling—Net Primary Productivity (NPP)

Aboveground annual grassland productivity was determined at the height of the annual growing season in April 1997. Tree biomass was not sampled because of its sparse areal extent on the study site. Clip-plots (20 by 50 cm; 0.1 m^2) were collected to bare soil and sorted according to live species composition (biomass) and litter. Plant material was dried at 65°C for 48 h and weighed. The NPP for 1997 was determined as grams of biomass per square meter at each sample location. Duplicate plots were placed 1 m above each of 20 pit faces to correlate NPP with soil properties along the hillslope. All sample sites were geo-referenced with the Trimble GPS described above. Data from the nine soil pit locations are used here.

Statistical Analysis and Soil–Landscape Modeling

Statistical summaries, exploratory data analysis, and statistical modeling for derivation of quantitative soil–landscape models were accomplished using the Splus statistical analysis package (Mathsoft, 1999). Regression based soil–landscape models of A horizon depth, soil depth, C_{mass}, and NPP were developed. We use models of A horizon depth and soil depth to provide initial approximations of the soil–landscape structure across the catena hillslope [Albic (E) horizons do not exist on this hillslope]. The A horizon is the most biologically active layer where most soil C is stored. Its thickness is indicative of biological activity, but it also provides clues to the location of erosion and deposition on the hillslope. Soil depth, defined here as the depth of the overall A horizon plus B horizon(s), provides an indication of water storage capacity, nutrient storage pools, overall productivity, and longer-term erosion, deposition, and soil building processes. Overall, these variables provide a basis for hypothesizing the spatial distribution of process zones and landscape function. Finally, we develop spatial models of C_{mass} and NPP to represent the distribu-

Table 1. Soil measurements, site data and U.S. soil taxonomy classifications for sampled sites.

			<2 mm size fraction										Total sample		Total profile and site data characterization			
Pit	Hor.	Lower horizon depth	Clay	Silt	Sand	Silt/clay	Texture class	Organic C	N	pH (H_2O)	CEC†	Base saturation	Gravel	Bulk density	A horizon depth	Soil depth	Profile C_{mass}	Site NPP‡
		cm	%					%			cmol kg^{-1}	%		g cm^{-3}	cm		g cm^{-2}	g m^{-2}
1	A	3	27.7	33.6	38.7	1.40	CL	2.26	0.27	6.6	27.1	92	33.3	0.95	16	34	56	319
1	AB	16	27.3	33.4	39.3	1.44	CL	2.08	0.25	6.5	27.7	92	30.8	1.84	Typic Xerorthent			
1	BAt	34	30.1	31.4	38.5	1.28	CL	1.39	0.20	6.6	25.8	93	48.7	1.36				
2	A	3	28.4	33	38.7	1.36	CL	1.61	0.20	6.5	24.2	87	35.3	0.9	28	85	63	200
2	ABt1	14	23.9	37.1	38.9	1.63	L	1.88	0.24	6.3	21.6	85	33.8	1.87	Typic Argixeroll			
2	ABt2	28	27.2	35.7	37.2	1.37	CL	1.12	0.17	6.4	22.8	89	50.8	1.65				
2	Bt1	45	42.2	13.2	44.6	1.06	C	0.64	0.15	6.3	37.2	88	34.4	1.65				
2	Bt2	85	37.7	13.9	48.4	1.28	SC	0.42	0.13	6.3	33.9	89	60.1	1.65				
4	A1	6	25.2	41.3	33.5	1.33	L	2.12	0.25	6.3	22.6	85	19.6	0.72	31	120	115	548
4	A2	17	26.4	40.2	33.4	1.27	L	1.14	0.17	6.4	20.7	86	28.6	1.95	Typic Argixeroll			
4	AB	31	26.9	38.9	34.1	1.27	L	2.15	0.24	6.4	21	87	26	2.01				
4	Bt1	52	47.4	32.3	20.3	0.43	C	0.57	0.14	6.3	39.7	89	24.3	1.65				
4	Bt2	80	39	36.1	25	0.64	CL	0.36	0.12	6.6	35	92	22.2	1.63				
4	Bt3	120	36	45.4	18.5	0.51	SICL	0.24	0.15	6.9	35.4	93						
8	A1	4	25.4	28.5	46.1	1.81	L	2.26	0.26	6.6	25	92	36.2	1.6	16	48	39	143
8	A2	16	27.8	27.3	44.9	1.62	CL	1.65	0.22	6.3	25.2	88	37.6	1.6	Mollic Haploxeralf			
8	Bt	48	50	13.9	36.1	0.72	C	0.62	0.15	6.3	37.9	87	73.4	1.85				
10	A1	5	25.2	38.9	36	1.43	L	4.14	0.39	6.9	30.5	92	59.5	1.048	78	NA	195	826
10	A2	30	28.8	38.5	32.7	1.14	CL	1.78	0.23	6.7	26.5	90	35.6	1.591	Pachic Haploxeroll			
10	AB1	53	34.1	34.8	31.1	0.91	CL	0.87	0.15	6.8	29.3	89	37.2	1.41				
10	AB2	78	35.3	34.7	30	0.85	CL	0.67	0.13	6.9	29.2	91	30.6	1.685				
10	BA	113	36.4	33.7	29.9	0.82	CL	0.58	0.12	6.9	31.7	91	31.4	1.543				
10	B1	162	35.6	35	29.3	0.82	CL	0.42	0.11	7.1	30.4	91	37.5	1.52				
10	B2	205	34.9	34.4	30.7	0.88	CL	0.35	0.11	7.2	31.5	93	37	1.55				
10	BC	300	33.3	35.8	30.9	0.93	CL	0.23	0.09	7.3	32.4	92	32.5	1.59				
12	A1	3	36.3	42.5	21.2	0.58	CL	2.00	0.23	7	35.1	88	21.2	1.6	8	8	10	129
12	A2	8	39.2	40.3	20.5	0.52	CL	1.19	0.19	6.8	36.7	98	17.1	1.7	Typic Xerorthent			
14	A1	5	29.6	40.5	29.9	1.01	CL	2.61	0.29	6.8	29.6	92	45.3	1.2	63	365	192	337
14	A2	16	29.6	42.9	27.4	0.93	CL	1.63	0.22	6.6	28.5	89	38.5	1.4	Pachic Haploxeroll			
14	A3	32	32.7	41.6	25.6	0.78	CL	1.24	0.17	6.6	29.3	97	27.6	1.63				
14	AB	63	38.8	36.2	24.9	0.64	CL	0.91	0.15	6.7	33.7	95	39.7	1.69				
14	BA1	92	44.2	31.6	24.2	0.55	C	0.64	0.13	6.7	37.9	91	29.8	1.73				
14	BA2	130	39.7	34	26.3	0.66	CL	0.46	0.11	6.9	35.3	92	32.5	1.78				
14	B1	176	38.4	34.2	27.4	0.71	CL	0.32	0.10	7.1	35.5	89	36	1.68				
14	B2	365	37.5	35.1	27.4	0.73	CL	0.23	0.09	7.3	35.6	94	33.5	1.64				
18	A1	3	30.3	42.4	27.3	0.90	CL	1.16	0.17	7.3	33.2	93	27.8	1.64	80	160	115	309
18	A2	7	30.2	42.5	27.2	0.90	CL	1.34	0.19	6.9	32.5	94	22.6	1.57	Pachic Haploxeroll			
18	A3	42	32.8	39.2	28	0.85	CL	1.16	0.17	6.9	31.9	88	30.1	1.62				
18	AB	66	35.5	39.1	25.4	0.72	CL	0.74	0.13	7.2	33.8	92	22.6	1.63				
18	BA	90	35.6	39.6	24.8	0.70	CL	0.61	0.12	7.3	33.9	90	34.2	1.63				
18	B1	126	35.2	39.7	25.1	0.71	CL	0.48	0.11	7.5	33.9	92	27.6	1.63				
19	A1	5	26.8	42.5	30.7	1.15	L	3.87	0.36	6.5	29.7	83	46.3	1.2	45	457	204	636
19	A2	24	28.4	43	28.6	1.01	CL	1.67	0.18	6.7	28.1	93	40.1	1.45	Pachic Haploxeroll			
19	A3	40	31.2	40.3	28.5	0.91	CL	1.31	0.15	6.7	28.7	94	29.3	1.62				
19	AB1	80	39.2	35.8	25	0.64	CL	0.94	0.13	6.8	32.5	92	34.1	1.83				
19	BA/B1	122	39.7	32.7	27.6	0.70	CL	0.58	0.10	7.1	35.3	92	58.7	1.87				
19	B2	158	35.8	34.1	30.2	0.84	CL	0.42	0.09	7.2	32.9	94	43.6	2.06				
19	B	300	31	32.1	36.9	1.19	CL	0.21	0.08	7.3	29.9	93	46.5	1.71				
Min.			23.9	13.2	18.5	0.43		0.21	0.08	6.3	20.7	83	17.1	0.7	8	8	10	129
Max.			50.0	45.4	48.4	1.81		4.14	0.39	7.5	39.7	98	73.4	2.1	80	457	204	826
Mean			33.5	35.5	31.0	0.97		1.19	0.17	6.8	30.8	91	35.8	1.6	41	160	110	383

† CEC is cation-exchange capacity.
‡ NPP is net primary productivity.

tion of C in the soil and in the aboveground biomass and compare them with the soil property models.

Empirical regression models were developed using correlations between the response variables (A horizon depth, soil depth, NPP, C_{mass}) and the corresponding quantitative terrain attributes (explanatory variables) computed for each sample site location. Scatterplot matrices (Cleveland, 1993; Moore et al., 1993) were used for exploratory data analysis to complement forward and backward stepwise regression searches for useful combinations of predictor terrain attributes. The regression searches employed the Akaike Information Criterion (Akaike, 1974), which develops a statistic using the residual deviance penalized by the number of parameters requiring estimation in a model fit. Model fits were then developed and intercept terms, regression model coefficients, and goodness of fit parameters were output. Due to the small sample number, only linear relationships were used for modeling. The intercept term and regression coefficients were used to create prediction surfaces for the response variables using grid-based map algebra tools.

RESULTS

Soil Taxonomy Classifications

Table 1 provides background characterization data for the nine sampled soil pits along with integrated measurements (A horizon depth, soil depth, C_{mass}, NPP) and U.S. soil taxonomy classifications. Three soil orders (Entisols, Alfisols, and Mollisols) were identified on the catena hillslope all with Thermic temperature and Xeric moisture regimes. The concave positions are Pachic

Haploxerolls (Pits 10, 14, 18, and 19). The convex positions are Typic Xerorthents (Pits 1 and 12) and a Mollic Haploxeralf (Pit 8). Pits 2 and 4 are located in more stable shoulder landscape positions and are classified as Typic Argixerolls.

The distribution of soil classes suggests three topographically driven pedogeomorphic process zones: (i) concave areas dominated by processes of accumulation or gain of water and sediment (Pits 10, 14, 18, and 19 all have pachic epipedons), (ii) convex areas dominated by losses of sediment and water (Pits 1 and 12 have no significant diagnostic horizons and pit 8 is also quite weakly developed), and (iii) a relatively stable shoulder area dominated by in situ soil forming processes such as vertical translocation (Pits 2 and 4 have strong argillic and mollic diagnostic horizons, and pit 8 has a weakly developed argillic horizon).

Hillslope Data Synthesis

The soil texture classes from Table 1 show a generally uniform distribution of clay loam textures with slightly coarser textures toward the profile surface. Change in clay percentages down the soil profile suggests pedogenic eluviation–illuviation processes, particularly in the upper slope profiles. The concave profiles appear well mixed. Silt percentages are generally highest in the surface horizons and there is more silt in the lower landscape positions. Sand values are greatest in upper landscape positions. Gravel percentages are greater in the surface of the two mid-slope concave (Pits 10 and 14) positions than elsewhere, suggesting past high-energy erosional events or proximity to steep sideslopes. Gravel is also greater in the deeper horizons of soils in upper hillslope positions because of parent material weathering and mixing. Sand/clay ratios are greater in convex and shoulder hillslope pits because of a combination of down-profile and downslope removal of finer materials. Bulk densities are greater in the lower A horizons of upper slope positions than in concave positions. This suggests greater water storage capacities in concave positions because of increased pore space and soil depth.

Soil pH is generally neutral in the deeper horizons of concave landscape positions, which can be explained by the downslope and down-profile increase in base cations (Table 1). Cation-exchange capacities follow clay content and cluster around 30 $cmol_c\ kg^{-1}$. If we assume average clay content of 30%, the CEC of the clay fraction would be around 100 $cmol_c\ kg^{-1}$, which suggests the presence of 2:1 clay minerals in all landscape positions. Table 2 shows the correlation coefficients among chemical and physical properties presented in Table 1. As expected, clay content is highly correlated with CEC, whereas soil organic C and N are negatively related to clay and bulk density.

Table 2. Matrix of correlation coefficients (*r*) between measured soil physical and soil chemical properties from nine soil pits.

Soil variables	Clay %	Sand %	Silt %	Gravel %	Bulk density
Org. C%	−0.66	0.28	0.29	0.10	−0.51
N%	−0.63	0.31	0.23	0.08	−0.53
pH(H_2O)	0.15	−0.48	0.35	−0.12	0.13
CEC†	0.87	−0.52	−0.23	0.02	0.25
% Base Sat.	0.20	−0.36	0.18	−0.13	0.17

† CEC is cation-exchange capacity.

Figure 2 shows depth distributions of organic C and N. The plots are organized roughly equivalent to the geographic locations of each pit on the hillslope (i.e., plots on top represent upper hillslope positions). The plots show that C and N decrease with depth, and the surface horizons in pits on concave slope positions (Pits 10, 19, and 14) contain the greatest amount of C and N. Figure 3 is a depth plot of the log transform of the C/N ratio for all sample points on the hillslope. Linear regression lines separate two visually apparent subsets that show different trends; Pits 1, 2, 4, 8, and 12 show a negative depth relation that is not as steeply sloping as for Pits 10, 14, 18, and 19. More fresh organic C has accumulated in concave landscape positions, which may be due to larger water-holding capacity and lateral redistribution of water into these landscape positions providing relatively favorable conditions for plant growth and NPP. Alternatively, it may indicate downslope movement of relatively fresh organic matter from convex positions.

Soil–Landscape Modeling

Figure 4 shows a scatterplot matrix with smooth fits illustrating relationships between each of the response variables (soil depth, A horizon depth, C_{mass}, NPP) and the CTI calculated at different DEM grid-point spacings. In all cases, the response variable increases with increasing CTI indicating that they respond positively to increasing concavity and flow accumulation. Even though the sample number is small, the scatterplots show predictive relationships that hold across DEM resolutions of 2 to 10 m, although the range of CTI on the abscissa shifts to larger values and is more restricted as the grid-point spacing increases. This is due to the sequential flattening of topography with larger grid-point spacings as previously documented by Gessler (1996). Similar scatterplot matrices were developed for each potential explanatory terrain variable to provide a visual complement to the stepwise regression search process. This exploratory analysis identified the 2-m resolution as most useful because of the statistical strength of the relationship and the finer representation of topographic variation. Table 3 lists the best statistical models derived from the search for predictive relationships between the response variables and all possible combinations of terrain attributes calculated at 2-m grid-point spacing.

A horizon depth is best predicted by use of slope, flow accumulation, and the CTI terrain variables (Table 3). This strongly suggests that lateral movement of water and sediment as differentiated by the local-slope and upslope contributing area are key processes contributing to A horizon thickness. Although the combination of these terrain variables provided the best model (Table 3, Model 1), each of the contributing model coefficients are highly correlated. A simpler model using only the CTI provides a lower correlation coefficient, but still

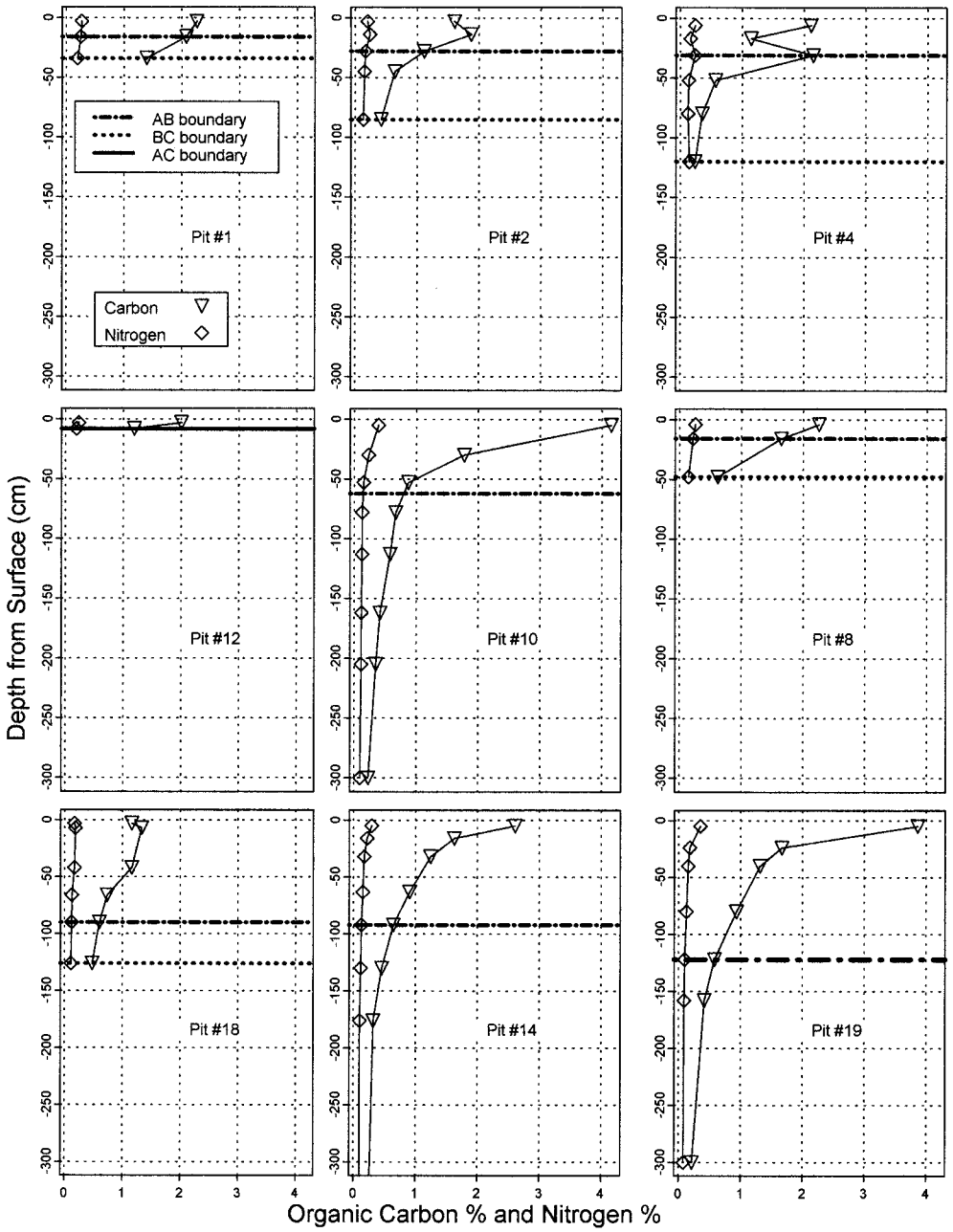

Fig. 2. Organic C percentage and N percentage depth plots with major horizon breaks for subset of nine soil pits selected for sampling.

accounts for 71% of the A horizon variation. This is a very powerful relationship given the small number of samples.

The best model for soil depth combined the CTI with upslope mean profile curvature. Profile curvature is the rate of change of slope in a downslope direction. It characterizes changes in flow acceleration that may differentiate erosion and deposition zones in landscapes. The upslope mean profile curvature variable therefore provides a quantification of relative erosional vs. depositional contributing areas. The correlation between the model coefficients of CTI and upslope mean profile curvature is only 0.37, suggesting that they provide complementary explanatory utility in the model (Table 3, Model 3). However, the simpler model using CTI alone results in an R^2 of 0.84, a very strong and easily derived correlation useful for modeling soil depth across the hillslope catena.

The two best models for NPP use CTI and flow accumulation as single linear predictors. Correlations are not as strong as for other variables. The scatterplots in Fig. 4 suggest that the relationship may be stronger at small CTI values but that the residual variance increases with larger CTI values when modeled with a linear fit. A much larger sample or alternative statistical methods that account for changes in residual variance would be required to test this hypothesis. The use of the flow-accumulation attribute implies that lateral redistribution of water in these landscapes results in higher plant productivity.

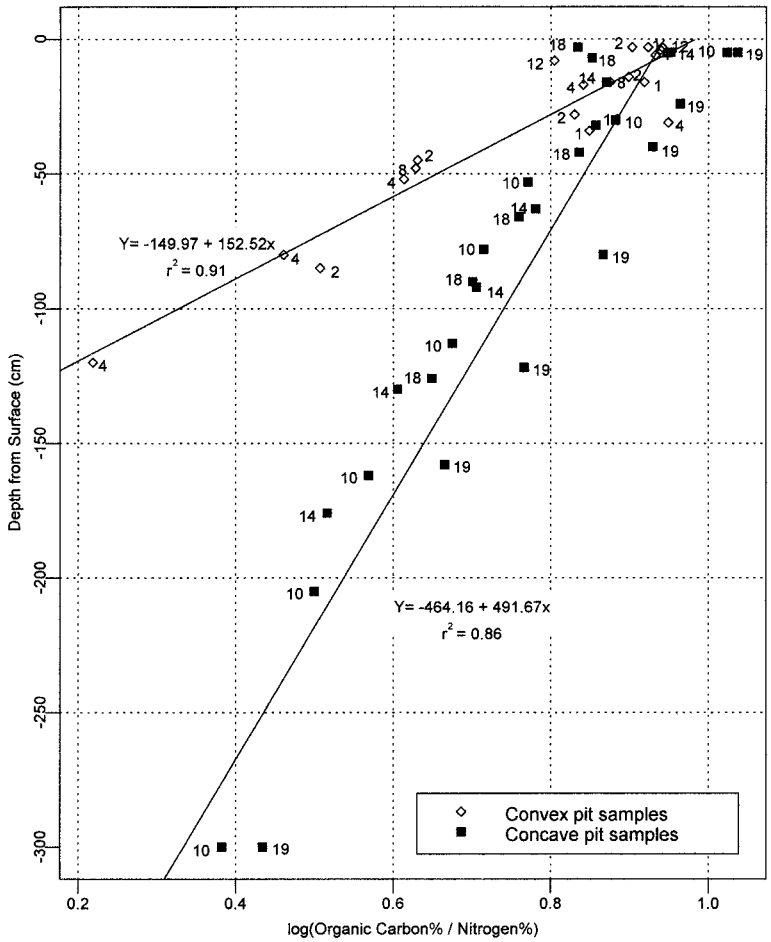

Fig. 3. Log organic C/N ratio depth plots and linear regression model fits to two visually distinct soil pit sample subsets. Numbers next to the sample points represent the soil pit from which the sample was collected.

The best models for profile total C are derived by combinations of slope and flow accumulation. The combination of these individual variables provides only a slight improvement on a model using the CTI alone. This predictive relationship is very strong as suggested by the scatterplots in Fig. 4, accounting for 78% of the variation in C stored in the soil of this catena. The amount of soil C stored in the soil profile is probably the result of both plant productivity and lateral redistribution of materials over the hillslope. Again, this relationship emphasizes the potential for quantitative modeling of C_{mass} using easily derived digital terrain attributes.

Spatial Implementation

Model coefficients and intercept terms from Table 3 were used to implement models for the 2-m grid point DEM using map algebra to provide predicted surfaces for each of the four predicted soil–landscape variables (Fig. 5). The four predicted surfaces follow pedologically logical patterns as concavity increases in the downslope direction. The regression model patterns vary smoothly without abrupt changes except as an artifact along the footslope of the catena where sampling was minimal. Regression models inherently smooth information; implementation of different model types such as decision trees can produce much sharper boundaries (Gessler, 1996). Catena topography follows relatively smooth transitions that are well represented by regression models.

DISCUSSION

Soil survey maps covering the study area show a single Chamise series map unit for the study site. Our detailed investigation found Entisols, Mollisols, and Alfisols representing separate zones of net loss, net gain, and relative stability on this 2-ha hillslope. The distribution of cation exchange capacity, base cations, and bulk density reflect these processes and further suggest that the concave regions of the hillslope have characteristics that are more favorable to plant growth and net primary production. Higher C and N values in the concave-position soil profiles indicate that NPP is greater in these zones perhaps due to exploitation of accumulated moisture.

A horizon depth varies from 8 to 80 cm and soil depth varies from 8 to >450 cm across the hillslope. This variation occurs within 10 to 15 m of horizontal distance representing changes in soil properties that could never be incorporated into a soil survey map at standard cartographic scales (i.e., 1:15 840; 1:20 000). A horizon depth

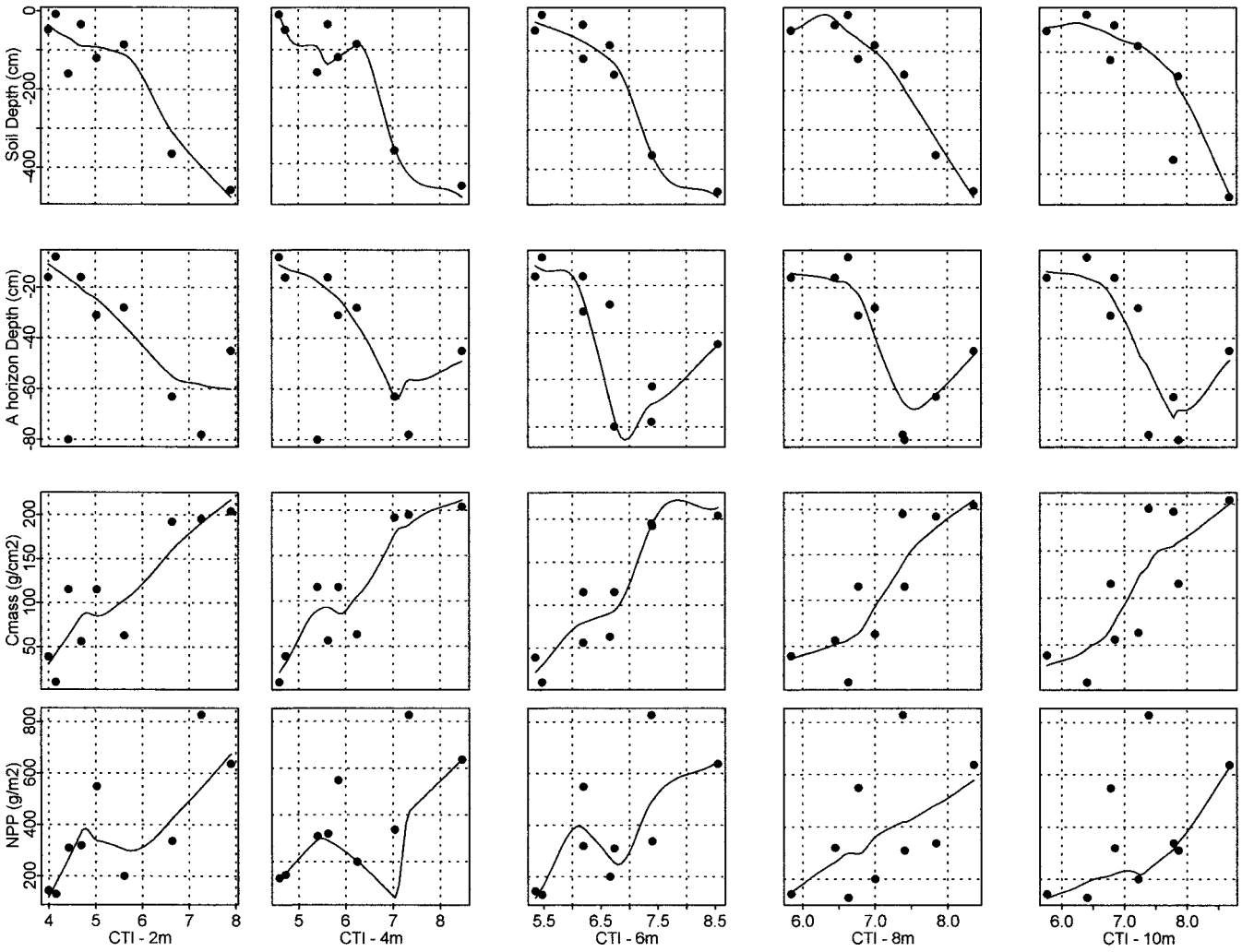

Fig. 4. Exploratory scatterplot matrix and local regression smoother fits for four measured soil properties vs. varied grid-spacing resolution CTI terrain variable.

and soil depth result from an integration of pedogeomorphic processes through time. A horizon depth may be more indicative of an integration of shorter-term processes relating to recent surficial dynamics and biotic activity. Soil depth represents a longer-term integration of processes that could include more than one event of A horizon development and/or the dynamics of A horizon gains and losses along with the deeper weathering of parent materials and hydrological dynamics. The A horizon and soil depth soil–landscape models are

Table 3. Soil–landscape models with regression coefficients and model fit statistics.

	Multiple regression models Explanatory terrain variables and regression coefficients†					
Predicted variable	**Intercept term**	***b* variable 1**	***b* variable 2**	***b* variable 3**	R^2	***P* value**
1. A-horizon depth	**1272.55**	**−13.55 slope****	**437.58 log(flowacc)****	**−432.56 cti****	**0.85**	**0.0163**
2. A-horizon depth‡	**−44.89**	**14.23 cti****			**0.71**	**0.0085**
3. Soil depth	**−383.21**	**120.83 log(flowacc)****	**−40.42 upprf NS§**		**0.88**	**0.0048**
4. Soil depth‡	**−429.73**	**111.12 cti****			**0.84**	**0.0013**
5. NPP¶	**−319.10**	**127.16 cti***			**0.58**	**0.0173**
6. NPP‡	**−285.15**	**135.08 log(flowacc)***			**0.52**	**0.0278**
7. C_{mass}	**−47.76**	**−1.83 slope NS**	**43.02 log(flowacc)****		**0.80**	**0.0076**
8. C_{mass}‡	**−141.24**	**45.58 cti****			**0.78**	**0.0015**

*** Significant at the 0.05 probability level.**
**** Significant at the 0.01 probability level.**
† Explanatory terrain attributes computed from 2-m grid spacing source DEM: slope = slope percentage; flowacc = contributing flow accumulation or watershed area; cti = compound topographic index; upprf = upslope mean profile curvature.
‡ Model used for implementation in Fig. 5.
§ NS is not significant.
¶ NPP is net primary productivity.

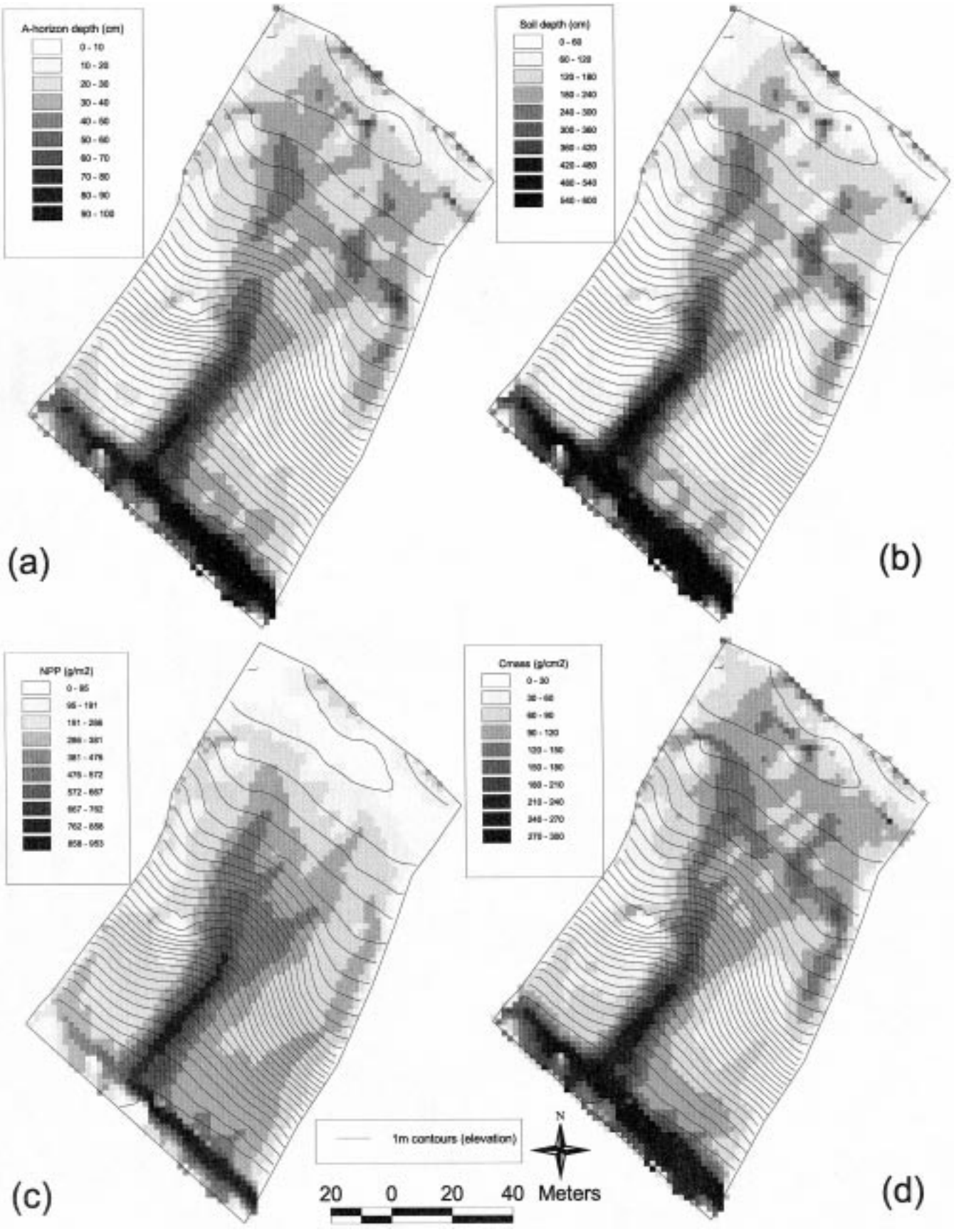

Fig. 5. Predicted soil–landscape model surfaces implemented from predictive models as indicated in Table 3.

similar to other work in Australia (Gessler, 1996) where soil depth was more predictable than A horizon depth using a similar set of explanatory terrain variables. The results here suggest that external landform is an important modifier of long-term landscape processes and should be explicitly incorporated into biogeochemical cycling models for this region. The weaker relationship between A horizon depth and external landform suggests that shorter-term processes are more random and variable.

The distribution of soil C along the catena is well represented by our models; there is more C in the deeper soils in the downslope concave positions. We noted that the C/N ratios for the soil profiles split into an upslope, smooth to convex grouping, and a downslope concave group. The plots implied greater addition of relatively fresh C to the latter group. If C accumulation is favored on some parts of the catena compared with others, how does the C_{mass} in the diversity of hillslope positions compare with that on a flat surface that is less subject to mass and water movement? Is more C sequestered in the concave positions than is lost from the convex positions by erosion? We tried answering this question by measuring C_{mass} in soil on the planar terrace top whose morphology is very similar to those on the upper shoulder positions (argillic and mollic diagnostic horizons). Calculation of C_{mass} using the same methods outlined above gives an estimate of 121 g cm^{-2} for the ridgetop. Comparing this value with those listed in Table 1 indicates loss sites (Pits 1, 2, 4, 8, and 12), and gain sites (Pits 10, 14, 18, and 19), matching those differentiated by the two separate regression lines illustrated in Fig. 3. The average C_{mass} for the sample sites across the hillslope is 110 g cm^{-2}. This suggests a relatively small loss of C on the hillslope compared with the ridgetop if we use simple spatial averaging. On the other hand, because the C_{mass}-landscape model incorporates CTI, it provides a more appropriate representation of the spatial variation of C_{mass} and produces a landscape-weighted average value of 99 g cm^{-2}, suggesting a greater net loss of C on the hillslope compared with the ridgetop. We do not wish to overinterpret this back-of-the-envelope calculation, but these initial estimates provide comparative values helpful in development of more rigorous mass balance monitoring.

Aboveground net primary productivity provides a measure of robustness for short-term biotic processes that integrate water balance and nutrient availability, in contrast to C_{mass}, which is a result of longer-term mass balance in landscapes. The NPP landscape model was less reliable than the others for various possible reasons. First, plants have an inherent plasticity in their response to environmental variation. Second, subtle changes in species composition with microtopography may alter NPP in poorly understood ways. Finally, while trees were relatively sparse on the catena, their exclusion from our measurement protocol limits our interpretive ability.

Although the modeling focused on use of terrain attributes computed at 2-m grid spacing, exploratory data analysis suggested that the functional relationships hold at broader gridpoint spacings. The range of each potential explanatory terrain attribute constricts with increases in grid spacing. Implementation of the model coefficients and intercept values for spatial prediction in some instances produced negative and unrealistic values. However, extrapolation beyond the range of the explanatory variables generated nonrealistic values. In scaling models to other areas, it is important to sample the entire range of explanatory variables during model development. Future research needs to evaluate these issues carefully as they relate to extrapolation of developed models.

Implications for Modeling Soil–Landscape Function and Process

Our results show a tremendous amount of variation in basic soil properties that strongly influence C distribution and dynamics in this 2-ha catena. This variation relates strongly to landform as shown by comparative evaluation of soil classes, soil physical and chemical data, and measurements of A horizon depth, soil depth, and net primary production and mass of C stored in the soil profile. Our sample size was small—a constant problem in pedology. Yet, correlation of soil properties with digital terrain attributes (landform) can be quantified statistically and applied with a GIS to predict values across landscapes. Our procedures provide explicit and quantitative models that can be tested, updated, and used for testing hypotheses about the spatial distribution of landscape and ecosystem processes. They can also be used for parameterizing spatially distributed hydrological and ecosystem simulation models to help understand landscape dynamics that drive biogeochemical cycling.

Soil processes controlling C content and flux are complex. They are usually studied in detail locally and extrapolated using simulation approaches. Regional to global distribution of soil C content and turnover are often estimated using simulation models that are based on a few easily measured soil and ecosystem parameters (e.g., the CENTURY model, Parton et al., 1987). Simulation models provide greater flexibility than earlier approaches where properties and processes measured in broadly defined ecosystems are scaled up using global maps of ecosystem distribution (e.g., Ajtay et al., 1979; Post et al., 1982). Inherent in the simulation model approach as implemented by CENTURY is the assumption that climate controls vegetation distribution which in turn controls soil C properties. Macroclimate is assumed the dominant control on soil C dynamics. In flat to gently sloping terrain, this is probably valid, but in most hillslope areas there is considerable redistribution of water by overland flow or subsurface flow. On hillslopes, local differences in soil processes related to differences in topographic position are underestimated. The effect of landscape topography is an important missing component in simulation models.

Ignoring the effect of topography on ecosystem processes introduces a serious weakness in present approaches to regional and global C modeling and proba-

bly exacerbates our inability to account for all the sinks of anthropogenically produced C. Water distribution in landscapes tightly controls soil C dynamics. In fact, water redistribution between convex and concave landscape positions, as demonstrated here, may account for differences in soil C similar to dramatically different climatic zones. Topography and its influence on hydrology and soil C dynamics has been difficult to quantify because of the continuously varying nature of hillslopes and our inability to sample and model the variation in a systematic fashion.

Through the power of digital elevation modeling implemented within a geographic information system, we can explicitly incorporate surficial processes into the hillslope context. To continue this effort we have instrumented the soil pits described here for monitoring soil water, gas, and temperatures fluxes over time. This will enable the testing of specific hypotheses about catenary soil–landscape function and biogeochemical cycling.

ACKNOWLEDGMENTS

The authors acknowledge support for this project from NASA and the University of California (California Space Grant). The authors thank Virginia Boucher, Mark Reynolds, Tomas Gotthold, Aaron Miller, and Josh Schimel for assistance in implementation of this study, and R. Dave Hammer and the Missouri Soil Analysis lab for sample analysis. The authors also thank an anonymous reviewer for helpful comments and suggestions.

REFERENCES

Akaike, H. 1974. A new look at statistical model identification. p. 716–722. IEEE Transactions on Automatic Control AU-19.

Ajtay, G.L., P. Ketner, and P. Duvigneaud. 1979. Terrestrial primary production and phytomass. p. 129–182. *In* B. Bolin et al. (ed.) The global C cycle. John Wiley and Sons, New York, NY.

Cleveland, W.S. 1993. Visualizing data. Hobart Press, Summit, NJ.

Conacher, A.J., and J.B. Dalrymple. 1977. The nine unit landsurface model: an approach to pedogeomorphic research. Geoderma 18:1–154.

Dikau, R. 1989. The application of a digital relief model to landform analysis in geomorphology. p. 51–79. *In* J. Raper (ed.) Three dimensional applications in geographical information systems. Taylor & Francis, London.

Gallant, J.C., and J.P. Wilson. 1996. TAPES-G: A grid-based terrain analysis program for the environmental sciences. Comput. Geosci. 22:713–722.

Geoprobe Systems. 1995. A percussion probing tool for the direct sensing of soil conductivity. Technical paper no. 94–100. Salina, KS.

Gessler, P.E., I.D. Moore, N.J. McKenzie, and P.J. Ryan. 1995. Soil–landscape modelling and spatial prediction of soil attributes. Int. J. Geogr. Info. Sys. 4:421–432.

Gessler, P.E. 1996. Statistical soil–landscape modeling for environmental management. Ph.D. thesis. Australian National University, Canberra.

Gessler, P.E., N.J. McKenzie, and M.F. Hutchinson. 1996. Progress in soil–landscape modeling and spatial prediction of soil attributes for environmental models. Proc. Int. Conf./Work. on Integ. GIS and Environ. Model., 3rd. Santa Fe, NM. 21–26 Jan. 1996. National Center for Geographic Information and Analysis. NCGIA. Santa Barbara, CA. http://www.ncgia.ucsb.edu/conf/SANTA_FE_CD-ROM/main.html.

Hole, F.D., and J.B. Campbell. 1985. Soil landscape analysis. Rowman & Allenheld, Totowa, NJ.

Holmes, K.W, O.A. Chadwick, and P.C. Kyriakidis. 2000. Error in a USGS 30-meter digital elevation model and its impact on terrain modeling. J. Hydrol. (Amsterdam) 233:154–173.

Hutchinson, M.F. 1989. A new method for gridding elevation and stream line data with automatic removal of pits. J. Hydrol. (Amsterdam) 106:211–232.

Hutchinson, M.F. 1996. A locally adaptive approach to the interpolation of digital elevation models. Proc. Int. Conf./Work. on Integ. GIS and Environ. Model., 3rd., NCGIA, University of California, Santa Barbara, CA. http://www.ncgia.ucsb.edu/conf/SANTA_FE_CD-ROM/main.html.

Mathsoft. 1999. S-PLUS 2000 user's guide. Data Analysis Products Division, Mathsoft, Seattle, WA.

McKenzie, N.J., P.E. Gessler, P.J. Ryan, and D.A. O'Connell. 2000. The role of terrain analysis in soil mapping. p. 245–266. *In* J.P. Wilson and J.C. Gallant (ed.) Terrain analysis: Principles and applications. Wiley, NY.

McSweeney, K., P.E. Gessler, B. Slater, D. Hammer, J. Bell, and G.W. Petersen. 1994. Towards a new framework for modeling the soil–landscape continuum. p. 127–145. *In* R. Amundson and J.W. Harden (ed.) Factors of soil formation: A fiftieth anniversary retrospective. SSSA Spec. Publ. 33. SSSA, Madison, WI.

Milne, G. 1935. Some suggested units of classification and mapping particularly for East African soils. Soil Res. 4:3.

Milne, G. 1936. Normal erosion as a factor in soil profile development. Nature (London) 138:548–549.

Moore, I.D., A.R. Ladson, and R. Grayson. 1991. Digital terrain modelling: A review of hydrological, geomorphological, and biological applications. Hydrol. Processes 5:3–30.

Moore, I.D., P.E. Gessler, G.A. Nielson. 1993. Soil attribute prediction using terrain analysis. Soil Sci. Soc. Am. J. 57:443–452.

Parton, W.J., D.S. Schimel, C.V. Cole, and D.S. Ojima. 1987. Analysis of factors controlling soil organic matter levels in Great Plains grasslands. Soil Sci. Soc. Am. J. 51:1173–1179.

Post, W.M., W.R. Emanuel, P.J. Zinke, and A.G. Stangenberger. 1982. Soil C pools and world life zones. Nature 298:156–159.

Simonson, R.W. 1959. Outline of a generalized theory of soil genesis. Soil Sci. Soc. Am. Proc. 23:152–156.

Smeck, N.E., E.C.A. Runge, and E.E. Mackintosh. 1983. Dynamics and genetics modeling of soil systems. p. 51–81. *In* L.D. Wilding et al. (ed.) Pedogenesis and soil taxonomy. I. Concepts and interactions. Elsevier, Amsterdam, the Netherlands.

Soil Survey Staff. 1993. Soil survey manual. USDA-Soil Conservation Service. Agric. Handb. 18. U.S. Gov. Print. Office, Washington, DC.

Soil Survey Staff. 1996. Soil survey laboratory methods manual. Soil Survey Investigations Rep. 42, Version 3.0. USDA-NRCS, Lincoln, NE.

Sommer, M., and E. Schlichting. 1997. Archetypes of catenas in respect to matter—A concept for structuring and grouping catenas. Geoderma. 76:1–33.

Speight, J.G. 1968. Parametric description of landform. p. 239–250. *In* G.A. Stewart (ed.) Land evaluation. Macmillan Co., Melbourne, Australia.

Trimble Navigation Ltd. 1996. TRIMMAP user's manual, Version 6. Sunnyvale, CA.

USDA, Soil Conservation Service. 1972. Soil survey of northern Santa Barbara County, CA. In cooperation with Univ. of California Agric. Experiment Station. U.S. Govt. Print. Office, Washington, DC.